the kinetic unit itself: the thermal coefficient of the frictional resistence that the immediate environment opposes to the rotation of the fluorophore and the amplitude of the fluorophore rotations at which its interaction with the protein environment becomes important. It demonstrates unequivocally the existence in peptides and proteins of fluorophore environments that differ greatly in these properties. These quantitative differences cannot be presently interpreted in terms of the motions associated to particular conformations of the molecules but do furnish data for the evaluation of future detailed calculations of the dynamics of proteins.

Registry No. Nuclease, 9026-81-7; chymotrypsin, 9004-07-3; tyrosine, 60-18-4; tryptophan, 73-22-3; lysozyme, 9001-63-2.

References

Ichiye, T., & Karplus, M. (1983) *Biochemistry 22*, 2884–2893.
Imoto, T., Forster, L. S., Rupley, J. A., & Tanaka, F. (1971) *Proc. Natl. Acad. Sci. U.S.A. 69*, 1151–1155.
Karplus, M., & McCammon, A. J. (1981) *CRC Crit. Rev. Biochem. 9*, 293–349.
Kasprszak, A., & Weber, G. (1982) *Biochemistry 22*, 5924–5927.
Lehrer, S. (1978) *J. Mol. Biol. 118*, 209–226.
Nicholas, P., Batelier, G., Rholam, M., & Cohen, P. (1980) *Biochemistry 19*, 3565–3573.
Rholam, M., & Nicolas, P. (1981) *Biochemistry 20*, 5837–5843.
Scarlata, S., Rholam, M., & Weber, G. (1984) *Biochemistry* (second paper of three in this issue).
Weber, G. (1952) *Biochem. J. 51*, 145–155.
Weber, G., Rholam, M., & Scarlata, S. (1984) *Biochemistry* (first paper of three in this issue).

Raman Spectroscopy of Homologous Plant Toxins: Crambin and α_1- and β-Purothionin Secondary Structures, Disulfide Conformation, and Tyrosine Environment†

Robert W. Williams* and Martha M. Teeter

ABSTRACT: The Raman spectrum of crambin crystals is different from the spectrum of crambin in solution. The amide I spectrum of crambin in solution is not different from the solution spectra of proteins homologous (>40%) with crambin, α_1- and β-purothionins. We have two interpretations of these results. One is that helical segments in crambin and the purothionins in solution are more irregular than those in crystalline crambin. Comparative analyses of amide I and amide III spectra, and of the conformational preferences of the amino acid sequences of these proteins, are consistent with this interpretation. The other is that, due to the way helical segments in crambin are stacked end on end along the same axis in the crystal, transition dipole coupling along the axis of these extended helixes enhances the amide I intensity of helical residues. On the basis of a combined Raman and sequence conformational analysis, we propose that the structure of the purothionins is the same as that of crambin in solution and that residues 7–12 in crystalline crambin are somewhat more regular and ordered than they are in solutions.

In this paper we describe the measurement and analysis of as small structural differences in proteins in crystals and solutions and with highly conserved amino acid sequences. We combine a quantitative Raman measurement of structure with an analysis of the secondary structure preferences of the protein sequences for crambin and two toxins, α_1- and β-purothionin. The crystal structure of crambin is known to a very high resolution by X-ray diffraction (Teeter & Hendrickson, 1979; Hendrickson & Teeter, 1981) and by neutron diffraction (Teeter & Kossiakoff, 1982). Therefore, we have also used this knowledge to make inferences about the structure of crambin and of the toxins in solution, which are compatible with the differences in the Raman spectra.

An analysis of how different amino acid sequences determine similar three-dimensional protein structures in the globins has been done by Lesk & Chothia (1980), but the effects of sequence differences on secondary structure were not emphasized. The conformational properties of amino acids in proteins have been analyzed [for example, see Chou & Fasman (1974), Robson & Suzuki (1976), and Levitt (1978)], but this important work has not lead to consistently accurate structure predictions.

One analysis of the accuracy of predictive methods shows that in four structure-type predictions based on sequence alone only 49% of the residue conformations are assigned correctly (Garnier et al., 1978). However, this same study concludes that if secondary structure content is known, 63% of all residues can be predicted correctly. The approach we take here combines accurate secondary structure estimates, an analysis of sequences, and a comparison with the known structure of crambin.

A method has been developed to quantitatively analyze the Raman amide I spectrum of proteins to obtain estimates of secondary structure content (Williams et al., 1980; Williams

† From the Biochemistry Department, Uniformed Services University of the Health Sciences, Bethesda, Maryland 20814 (R.W.W.), and the Department of Chemistry, Boston University, Boston, Massachusetts 02215 (M.M.T.). *Received November 2, 1983; revised manuscript received June 20, 1984.* This work was supported in part by NSF Grant PCM-8302893, ONR Grant WR30342, and USUHS Protocol 3I3R07139 to R.W.W. and by NSF Grant PCM 80-03929 and NIH Grant GM 30165 to M.M.T. Part of this work was performed at the Optical Probes Branch at the Naval Laboratory where R.W.W. was supported by a National Research Council research associateship.

0006-2960/84/0423-6796$01.50/0

& Dunker, 1981; Williams, 1983). This method is equally applicable to crystal, solution, and membrane-bound states of proteins. The standard errors for estimates of structure content are 3–6%, so for small proteins like the toxins it is possible to interpret with some confidence differences in the conformation of four or more residues. We have applied this analysis to a comparison of crystalline crambin with solutions of crambin and of the toxins, and we describe here our interpretations of differences between crystals and solutions.

Crambin is a hydrophobic, water-insoluble plant protein with no known biological activity (Van Etten et al., 1965). It can, however, be solubilized in water if included in phospholipid vesicles (Wallace et al., 1984). When crambin's amino acid sequence was determined (Teeter et al., 1982), it was found to be homologous to twelve plant toxins isolated from cereal grains (Mak & Jones, 1976a) and from mistletoes (Samuelsson et al., 1968). The plant toxins are hemolytic (Andersson & Johannsson, 1973), lyse a wide variety of cells (Okada & Yoshizumi, 1973; Carrasco et al., 1981), and cause skin and skeletal muscle contraction (Andersson & Johannsson, 1973). Lipids (Wooley & Krampitz, 1942) as well as metal ions (Okada et al., 1970) are known to prevent their toxic effects. Thus, something is known about the function of the plant toxins, but nothing beyond a primary sequence is known about their structures.

Crambin and the thionins have nearly identical lengths (46 and 45 amino acids, respectively), have the same disulfide bond linkages, with an additional disulfide in the purothionins, and have 40–50% sequence conservation. Thus, the three-dimensional structures of these proteins may be nearly identical, but until recently there has been no experimental evidence to support this assumption. Circular dichroisn (CD) spectra of crambin and the toxins in solution are similar (M. Whitlow, and M. M. Teeter, unpublished results). An analysis of the Raman spectra of crambin, a protein with a high-resolution three-dimensional structure, and a family of homologous toxins of unknown structure should present a model system to explore the potential for the prediction of three-dimensional structure from primary sequence and vibrational spectroscopy.

Materials and Methods

Samples of crambin were kindly provided by Drs. C. E. Van Etten and H. Tookey (Van Etten et al., 1965). Crambin crystals were prepared from 30 mg/mL solutions of protein in 80% ethanol in water, which were equilibrated against 60% ethanol by vapor diffusion (Teeter & Hendrickson, 1979). These crystals were later dried at 40 °C for 1 h and resuspended in water for another experiment and then dissolved in 100% ethanol and later made to 80% ethanol for solution experiments. Crystals were then precipitated from this solution by the addition of water for repeated Raman measurements.

Samples of crambin in methanol solutions were prepared by dissolving crambin in methanol and titrating with water until the crystals were formed at about 50% MeOH. These crystals were returned to solution by removing some of the supernatant above the crystals and titrating with methanol.

The purothionins were kindly provided by Dr. B. L. Jones and purification was as described by Mak & Jones (1976a,b) and Jones & Mak (1977). The purothionins were dissolved in 0.05 M phosphate–0.14 M NaCl, pH 7.1, and later made to 50% ethanol. The concentration of protein was about 5% by weight in the 50% ethanol.

The Raman instrumentation and method of amide I spectrum analysis for structure information are described elsewhere (Williams, 1983). Spectra were five-point smoothed (Savitsky & Golay, 1967). References proteins used in this work are the same as used earlier with two exceptions: (1) The spectral region used in the analysis is extended to 1710 cm^{-1}. (2) Estimates for the secondary structure of the reference protein avidin are modified as described by Honzatko & Williams (1982). The statistics that describe the agreement with X-ray structures do not change significantly when these changes are made.

The methods of amide III spectrum analysis are to be described in detail elsewhere (Williams, 1984). Briefly, the procedure is identical with that described for amide I spectra, but two different reference sets of amide III spectra are used.

One set, used to analyze the spectra in Figure 2, contains the amide III spectra of 13 proteins from 1225 to 1245 cm^{-1} and from 1275 to 1310 cm^{-1}. Correlation coefficients between Raman and X-ray estimates of helix and β-strand are 0.98 and 0.97, respectively, with this set.

The other set, used to analyze the spectrum in Figure 3, contains seven difference spectra. A reference difference spectrum is obtained when the spectrum of a deuterium-exchanged protein is subtracted from the spectrum of the same protein in water. When a protein has all of its amide protons exchanged with deuterium, the region from 1200 to 1330 cm^{-1} contains only those non-amide III bands that overlap with the amide III spectrum. When this spectrum, which contains only interfering bands, is subtracted from the spectrum of protein in H_2O, only the structurally sensitive amide III bands remain in the 1200–1330-cm^{-1} region. These interfering bands are also absent from the difference spectrum in Figure 3, so in principle the Figure 3 spectrum can be analyzed with the H_2O minus D_2O reference spectra. This was done as follows. The spectrum in Figure 3 was base-line adjusted and normalized so that the sum of the absolute values of intensities from 1225 to 1320 cm^{-1} was unity and the sum of intensities was zero. The difference reference set was fit to this spectrum with the unconstrained least-squares subprogram SVA. Crambin crystals were heated in D_2O at 90 °C for 24 h, and the spectrum of these crystals, show in Figure 2, was taken to approximate the spectrum of fully exchanged crambin. The friction of amide III intensity that is shifted in frequency due to structural changes was estimated by measuring the total area enclosed by the solid line and the solid line with the dot in Figure 2 (which is the difference between the amide III spectra of solid and solution crambin), dividing this value by 2, and then dividing the result by the area enclosed by the solid line and the dotted line (which is an estimate of the total amide III intensity), all between 1225 and 1320 cm^{-1}. The fractions of secondary structure obtained from the least-squares procedure were multiplied by this value, 0.12, to give the difference results in Table II.

We relied on the work of Siamwiza et al. (1975) in the interpretation of the tyrosine doublet between 820 and 860 cm^{-1}. In a similar vein, our analysis of the conformation of the disulfide bridges of crambin and α_1- and β-purothionin is based on the work of Van Wart & Scheraga (1976a,b).

Protein sequences were analyzed for the secondary structure information shown in Table III in the following way: A program was written (Honzatko & Williams, 1982) to average the preference values from Levitt (1978) for helix, β-sheet, and turn and from Chou & Fasman (1977) for turns. Values for helix and β-strand were obtained from a six- and four-residue average, respectively. The use of a run constant of 6 for helix has been described elsewhere (Garnier et al., 1978; Chou & Fasman, 1974). A run constant of 4 for β-strand was used here since the β-strands in crambin are four residues long. A run constant of 2 was applied to the turn preference values

Table I: Comparison of Secondary Structure Content (%) of Crambin α_1- and β-Purothionins from Amide I Spectra Using Two Least-Squares Methods

protein	method[a]	structure type[b]						totals	
		H_o	H_d	S_a	S_p	T	U	H	S
crambin crystal[c]	R1	33	14	23	3	16	11	46	26
	R2	26	13	28	1	19	13	40	28
	X-ray	28	17	22	0	22	11	46	22
crambin soln	R1	16	16	32	1	21	12	32	33
	R2	10	18	27	4	23	18	28	31
α_1-purothionin soln	R1	21	19	27	2	15	13	40	29
	R2	13	23	32	−4	19	16	36	28
β-purothionin soln	R1	19	18	31	0	16	13	37	31
	R2	10	22	34	−4	20	16	32	30
SD[d]	R1	4	4	5	3	3	3	7	4
	R2	4	4	5	4	3	3	5	3

[a] R1, eq 1 was solved with subprogram NNLS (Lawson & Hanson, 1974), which constrains solutions, x, to be positive. R2, eq 1 was solved with subprogram SVA (Lawson & Hanson, 1974), which allows negative solutions. X-ray values are from Hendrickson & Teeter (1981) except that two U's are reassigned to S_a as described under Materials and Methods. [b] H_o, ordered α-helix; H_d, disordered helix, correlated with the ends of helical segments, 3_{10} helix, or α_{II} (Nemethy et al., 1967) helix; S_a, antiparallel β-strands; S_p, parallel β-strands; T, turn as defined by Levitt & Greer (1977); U, undefined; H, total helix; S, total β-strand. [c] One residue = 2.2%. [d] The standard deviation is defined as $SD = ([\sum D_i^2 - (1/N)(\sum D_i)^2]/(N-1))^{1/2}$, where D_i = Raman $\%_i$ − X-ray $\%_i$ for each of $N = 14$ proteins in the reference set and where each protein being analyzed is exluded from the reference set.

from Levitt (1978) for two reasons: Many two-residue turns are found with the criteria of Levitt & Greer (1977). Also, the criteria applied by Hendrickson & Teeter (1981) to the crystal structure of crambin found two turns with two residues each.

We also used the 12 position-dependent β-turn preference values of Chou & Fasman (1977). These were averaged over each run of 12 residues. Averages greater than 1.17 were marked as turns in Table III only for the four residues in the β-turn positions. This analysis was included here for a comparison with the less sophisticated procedure using a run constant of 2.

Secondary structure was assigned to residues where the averaged perference values were highest, subject to the constraint that the number of residues assigned to each structure class must be equal, within the experimental uncertainty, to the number of residues estimated to be in that class by the Raman analysis. Priority conflicts between classes of structure were resolved by assigning turns first, followed by helix, and then β-strand, with no assignments being changed once they were made. Where β-strand residues could not be assigned in runs of four or more, the single residue preference values were used to assign β conformation to isolated residues. The crambin X-ray structure represented in Table I shows two more β-strand and two less undefined residues than that in Table II. This was done since residues 39–41 are in an approximately β conformation. This is consistent with the Levitt & Greer (1977) criteria for β-strand. The Levitt and Greer criteria assign an average of 7 ± 6% more β-strand to proteins than do others. This comes from a comparison of the X-ray secondary structures for nine proteins compiled in Williams (1983) with those in Chang et al. (1978).

Results and Discussion

The normalized Raman amide I spectra of crystals and solutions of crambin and α_1-purothionin in solution are compared in Figure 1. The β-purothionin spectrum is virtually identical with that of α_1-purothionin and is not shown. The spectrum of crambin in solution is not significantly different from the spectrum of the purothionins. However, the spectrum of crambin *in* crystals is quite different from these solution spectra.

Figure 1 also shows that this difference is not directly related to the polarity of the bulk solvent. The dielectric constant of

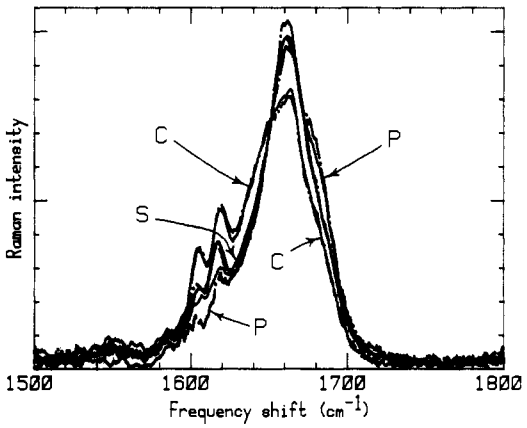

FIGURE 1: Comparison of Raman spectra of crambin crystals (C) in water (solid line) and 60% EtOH (line with dot), crambin solution (S) in 80% EtOH (solid line) and 100% EtOH (line with dot), and α_1-purothionin (P) in aqueous buffer (solid line) and 50% EtOH (line with dot). These spectra are normalized from 1600 to 1700 cm^{-1}.

the solvent may effect the amide I polarizability and, hence, the amide I intensity distribution. To test this possibility, we measured the amide I spectrum of each sample in a variety of alcohol concentrations. We observed no significant changes in the amide I spectra as a function of alcohol concentration alone. Crambin forms crystals at somewhere between 80 and 60% ethanol. α_1-Purothionin precipitates at greater than 50% ethanol, and the spectrum of precipitated purothionin is the same as that of purothionin in solution. (We have been unable to obtain spectra of the purothionins in the crystal phase.) It is possible that the removal of tightly bound water molecules during or near the crystal to solution phase transition may produce changes in the polarizability of amide groups at these sites, but whether or not these changes could be sufficient to change the amide I spectrum as seen here is an unanswered question.

Estimates of secondary structure content obtained from the amide I analysis are shown in Table I. The residual norms (root mean square errors) for the unconstrained fit (R2 in Table I) are less than half of what they are for the nonnegative fit (R1). For example, the residual norms for the fit of α_1-purothionin are 0.004 and 0.012 for R2 and R1, respectively. For this reason, we shall refer to the unconstrained solutions in discussion of the estimated secondary structure content. The

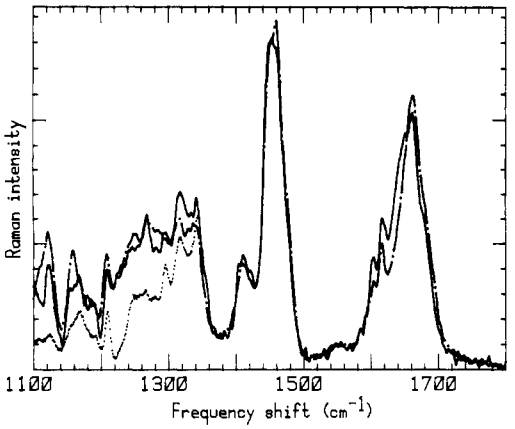

FIGURE 2: Comparison of Raman spectra of crambin crystals in 50% MeOH (solid line), crambin in solution at 90% MeOH (line with dot), and crambin crystals after 24 h at 90 °C in D_2O (dotted line from 1100 to 1350 cm^{-1}). These spectra are normalized from 1630 to 1700 cm^{-1}. The methanol CH band at 1450 cm^{-1} has been subtracted.

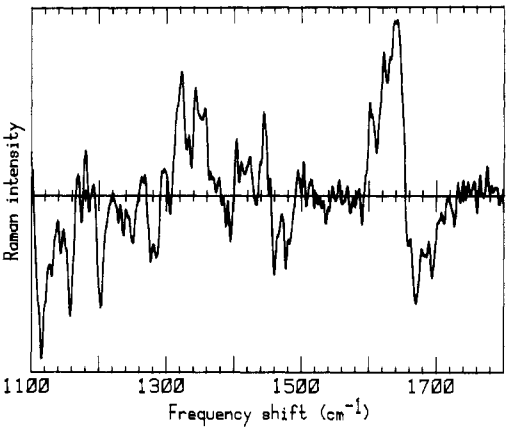

FIGURE 3: Difference spectrum of crambin crystals minus crambin in solution, from Figure 2. The sum of points from 1220 to 1340 cm^{-1} and from 1630 to 1700 cm^{-1} is approximately zero.

usefulness of these structure estimates is limited by their estimated standard deviations. We use the following criterion: two amide I derived structure estimates are different if they are more than two standard deviations apart. Under this condition, only one possible difference can be observed in Table I. There appears to be less ordered α-helix and more disordered helix in the purothionins and solution crambin than in crystalline crambin.

Disordered helix is defined here as including 3_{10} and α_{II} (Nemethy et al., 1967) helix and the helical residues on the ends of helical segments. A calculated spectrum of the disordered helix has two bands, one at 1658 cm^{-1} and one at 1682 cm^{-1} (Williams & Dunker, 1981). Ordered helix is defined as regular α-helix, although this definition is influenced in its application here by the dubious choice of helical poly(L-lysine) as a reference. A calculated spectrum of ordered α-helix has one band at 1642 cm^{-1}. The width of these bands is about 20 cm^{-1} (Williams & Dunker, 1981).

The current amide I analysis cannot, to some extent, distinguish between disordered helix and some types of turn (Williams, 1983). This may be due in part to the fact that a type III turn corresponds to one turn of a 3_{10} helix (Krimm & Bandekar, 1980). It is useful to compare the amide I bands of α_1-purothionin and insulin. The insulin reference spectrum is by far the largest single contributor to the fit of the purothionin spectra, and this is due probably to the band at 1680 cm^{-1}, which is intense for these proteins relative to the other proteins in the reference set. A vibrational analysis of insulin has provided evidence that much of the intensity near 1680 cm^{-1} can be assigned to β-turns (Bandekar & Krimm, 1980). It is also true that insulin contains more of what is defined here as disordered helix than other proteins (Williams & Dunker, 1981).

It may be possible that intermolecular transition dipole coupling between the helical segments in crystalline crambin shifts the affected amide I modes to lower frequencies. Transition dipole coupling may have relatively long-range effects (Moore & Krimm, 1976), and crambin molecules in the crystal are related by a 2-fold screw axis and a translation along the z axis so that helical segments in pairs of monomers run nearly parallel and are stacked end on end to form an extended helix made of segments about 6 Å apart. All of the amide I transition dipoles are aligned along the same axis. This would be an unprecedented example of how tertiary and quaternary structure information presents itself in the Raman spectrum.

Table II: Comparison of Secondary Structure Content (%) of Crystals and Solutions of Crambin from Amide III Spectra

spectrum	structure type[c] H_o	H_d	H	S	T
crystals[a]			51	25	
solution[a]			47	28	
crystals minus solution difference[b]	7	−3	4	−2	−2

[a] From Figure 2. NNLS was used to solve eq 1. The method and amide III reference spectra used here give significant results only for total helix and β-strand, with standard deviations of 5 and 6%, respectively. [b] From Figure 3. SVA was used to solve eq 1. The reference spectra used here were H_2O minus D_2O difference spectra as described under Materials and Methods. This method gives significant results for ordered helix, total helix, total β-strand, and reverse turn with standard deviations of 6, 9, 10, and 3%, respectively. These estimates are said to be significant here if the correlation coefficients for the comparison of Raman and X-ray estimates of structure for the reference proteins are greater than 0.8. H_d is included here for completeness, although it is not significant. [c] See Table I.

The amide III transition dipoles in these helical segments are not aligned. A difference between amide III spectra of crystals and solution of the same magnitude and direction as observed for amide I spectra could not be easily explained in terms of intermolecular transition dipole coupling.

The amide III spectra of crystalline and solution crambin are shown in Figure 2. When the spectrum of deuterated crambin is taken as the base line in the amide III region, the difference between the crystal and solution spectrum between 1220 and 1320 cm^{-1} corresponds to a 12% change. The change measured from the amide I band from 1630 to 1700 cm^{-1} is 8%. Thus, the changes in the amide I and III regions are about the same.

The difference spectrum in Figure 3 shows that the relative intensities of the amide I and III regions do not change between crystal and solution. If intermolecular transition dipole coupling is active in making the α-helical amide I bands more intense in the crystal than in the solution phase, we would not expect this to happen.

A secondary structure analysis of the amide III spectra in Figures 2 and 3 is summarized in Table II. Although the magnitude of the change seen here is not very significant in terms of the standard deviation in the structure estimates, these results show that the direction of the amide III change is toward less α-helix. The change in the actual spectrum is quite significant. The amide III secondary structure analysis is not adequately sensitive to detect the observed difference.

The idea that the crystal and solution conformations of a protein may differ has not been a serious concern for several

Table III: Comparison of Known Crambin Structure with Predictions for Secondary Structures of Crambin and Purothionins Using Combined Sequence and Raman Data

Sequence[a]				
number	1	2	3	4
crambin	TTCCPSIVARSNFNVCRLPGT$^{P}_{S}$GA$^{I}_{L}$CATYTGCIIIPGATCPGDYAN			
α_1-purothionin	KSCCRSTLGRNCYNLCRARG-AQKLCAGVCRCKISSGLSCPKGFPK			
β-purothionin	KSCCKSTLGRNCYNLCRARG-AQKLCAGVCKCKLTSGLSCPKDFPK			
Secondary Structure[b]	1	2	3	4
crambin, x-ray	////**000000000000***00000000-////***---**---			
crambin crystal[c]	////**//0000000000**-00000000//////**---**-/--			
crambin solution[c]	////**////0000000000**-**000000//////**---**-/--			
α_1-purothionin[c]	////////**00000000** 00000000//////***--****---			
β-purothionin	-///////**-0000000** 0000000//////**--**--**-			
12 position turn[d]	1	2	3	4
crambin		****		****
α_1-purothionin	*********	*** *		****
β-purothionin	******	*** *		
proposed model[e]	1	2	3	4
both purothionins	////???????0000000** *00000000-////**-/-**-//-			

[a] One-letter symbols. [b] (/) β-strand; (*) turn; (0) helix; (-) undefined. X-ray structure is from Hendrickson & Teeter (1981). [c] Predictions are made from combined sequence and Raman data as described under Materials and Methods. [d] Predictions are made from averaged 12-residue segments with the position-dependent preference values from Chou & Fasman (1977) with averages above 1.17 marked as "*". [e] (?) 3_{10} helix or turns.

years. The arguments against this possibility (Matthews, 1976) cite general thermodynamic evidence about the high solvent content and small surface contact of protein molecules in crystals, about the existence of proteins showing essentially the same crystal structure in several different space groups formed from radically different solvents, and that a number of enzymes are catalytically active in crystals. However, structurally different forms of pig insulin have been crystallized (Bentley et al., 1978). This alternative folding pathway for insulin may be important to its activity (Dodson et al., 1983).

Two recent studies show Raman amide I spectra of proteins in crystals and in solutions, nerve growth factor and avidin, which are essentially identical (Williams et al., 1982; Honzatko & Williams, 1982); however, other studies have found significant differences for other proteins. The amide I spectra of crystals at pH 4.5 and solutions at pH 7.2 of a 450-kDa multisubunit hemocyanin are significantly different (Williams & Hendrickson, 1984), possibly due to different subunit compositions or the different pH. Crystals and solutions of the 58-residue pancreatic trypsin inhibitor have similar amide I spectra (R. Williams, unpublished results). The amide I spectrum of the 26-residue protein melittin in crystals is different from the spectrum of melittin in physiological saline (R. Williams, unpublished results). The spectrum of insulin crystals at pH 7 is different from the spectrum of insulin solutions at pH 2 (Williams & Dunker, 1981), and the two crystal forms of insulin (Bentley et al., 1978) have different Raman spectra (R. Williams, unpublished results).

We have predicted secondary structure for each residue of α_1- and β-purothionin and crambin by using the estimates from Table I (R2) to constrain assignments made from the averaged conformational preferences of the amino acids. The results shown in Table III indicate the degree of success obtained when our simple criteria were applied to crystalline crambin.

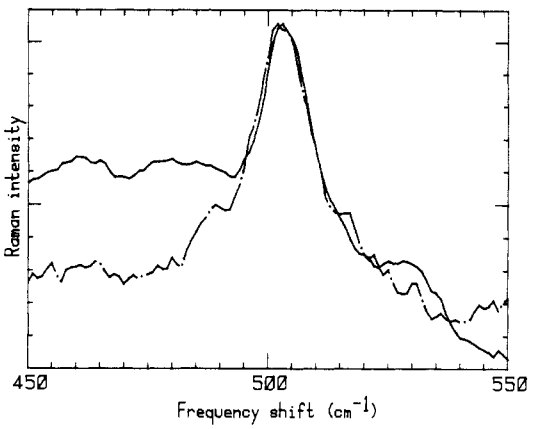

FIGURE 4: Disulfide Raman spectrum of crambin crystals (solid line) and α_1-purothionin (dash with dot) showing the strong disulfide band at 503 cm^{-1}.

While the uncertainty in this approach is great enough to preclude hopes for correctly assigning a four-class secondary structure to more than about 63% of the residues (Garnier et al., 1978), we propose that a comparison of the predictions for crystalline crambin with the purothionins and crambin in solution may implicate a region of sequence in connection with the differences observed in the amide I spectra. This hypothesis is made partly in order to provide grounds for a retrospective test of this approach after the crystal structure of one of the purothionins is solved.

The comparisons in Table III show that one region of the purothionin sequence is predicted by our criteria to differ in conformation from the corresponding crambin sequence, residues 5 through 11. The differences are due mostly to the preference value changes at residues 5 and 9 involving proline and glycine together with the cysteine at position 12 in the purothionins that forms a disulfide bridge, absent in crambin, to position 30 (crambin's numbering).

The significant difference between crystalline crambin and the purothionins in the amide I spectra involves only ordered and disordered helix (Table I). Helical residues 23–30 in crambin contain only three residues that may be assigned to the ordered class, and even though the matching residues in the purothionins may be disordered, this number is not sufficient to account for the estimates given in Table I. The helical segment 7–19 in crambin is both longer and more regular than 23–30 (Hendrickson & Teeter, 1981).

We propose that amino acids 5–11, part of which forms the regular α-helix in crystalline crambin, may be disordered in the purothionins and crambin in solution. This hypothesis is consistent with the differences observed in the amide I and III spectra. The difference may involve 3_{10} helix or turn structure in residues 5–11, but this is speculation since not enough is known about how relatively small purturbations in an α-helical structure may change the amide I frequency. Since a disulfide links residues 12 and 30 in the purothionins, this hypothesis is also consistent with the observation that there is seldom well-formed helix on both ends of a disulfide and that a frequent conformation at disulfide ends is a tight turn, a succession of turns, or a 3_{10} helix (Richardson, 1981).

The purothionins contain one more disulfide than crambin. This disulfide is between residue 12 and residue 30. Two of the three disulfides in crambin occur in the β-sheet region, and one occurs in the α-helix. If our prediction is corrent, the fourth disulfide connects the N-terminal of the first helix with the C-terminal of the second helix. Models have been built of purothionin, with the assumption that its secondary structure

Table IV: Dihedral Angles for Three Disulfide Bonds in Crambin

bond	angle (deg)[a]				
	χ^1	χ^2	χ^3	χ^4	χ^5
3–40	−52	−74	−80	−72	−65
4–32	−68	−80	105	−116	−56
16–26	179	−91	−87	−59	−65

[a] Angles: C_α χ^1 C_β χ^2 S_γ χ^3 S_γ χ^4 C_β χ^5 C_α.

was the same as crambin's (M. Whitlow and M. M. Teeter, unpublished results). In this case, the fourth disulfide would fall at the opposite end of the helices from the third disulfide. Connecting the sulfurs in this conformation involved only very small movements.

Figure 4 shows the disulfide stretching spectrum of crambin and α_1-purothionin. Van Wart & Scheraga (1976a,b) have shown with model studies that disulfide bonds with dihedral angles of 85 ± 20° have a band between 505 and 500 cm^{-1}. Disulfide bonds under conformational strain, with dihedral angles different from 85 ± 20°, have a band between 450 and 500 cm^{-1}. The disulfide bands for both crambin and α_1-purothionins are at 503 cm^{-1}, which is an ambiguous position with respect to the model studies. However, the disulfide dihedral angles for the three disulfides in crambin are known to a high precision and are given in Table IV (W. Hendrickson, personal communication). All three disulfide χ^3 dihedral angles are 85 ± 20°. This range of dihedral angles is observed in the majority of protein structures (Richardson, 1981).

Provided the S–S bond is not strained, the frequency of the stretching mode is sensitive to each of the two C_β–S dihedral angles, χ^2 and χ^4 in Table IV. The disulfide band at 503 cm^{-1} is consistent with results from model studies for C_β–S dihedral angles of 50–180°, and as can be seen in Table IV, the C_β–S dihedral angles in crambin are within this range. C_β–S dihedral angles of 0–50° give rise to a disulfide band near 540 cm^{-1}, and this has been observed in the Raman spectrum of avidin (Honzatko & Williams, 1982).

The disulfide band of α_1-purothionin is nearly identical with that of crystalline crambin, and no other distinct bands can be seen. From this it appears probable all of the four disulfides of α_1-purothionin fall into the category represented by Table IV.

Figure 5 shows the tyrosine doublet at 850 and 830 cm^{-1}. Siamwiza et al. (1975) have shown with model studies that the intensity ratio of these bands is sensitive to the hydrogen-bonding state of the phenolic OH. The 850-cm^{-1} to 830-cm^{-1} intensity ratio for both crambin and α_1-purothionin is about 10:6. This is consistent with an OH group that is hydrogen bonded to water, and indeed, the tyrosine OH groups on the surface of crambin are both hydrogen bonded to water molecules (M. M. Teeter, unpublished results). According to this evidence, the lone tyrosine of α_1-purothionin appears to be hydrogen bonded to water.

In summary, we have presented evidence consistent with the hypothesis that some of the helical residues in crambin are more ordered in crystals than they are in solution: Spectra of crystals and solutions are significantly different. Amide I spectra of homologous proteins in solutions are similar. structure estimates for ordered helix content in solution crambin are three standard deviations different from the X-ray value. Some of the evidence appears to be inconsistent with an alternative explanation for the amide I difference. Intermolecular transition dipole coupling along the crystal z axis, where helical segments are aligned end on end, may increase the intensity of the α-helix amide I bands relative to the rest of the spectrum. However, the amide I band does not appear

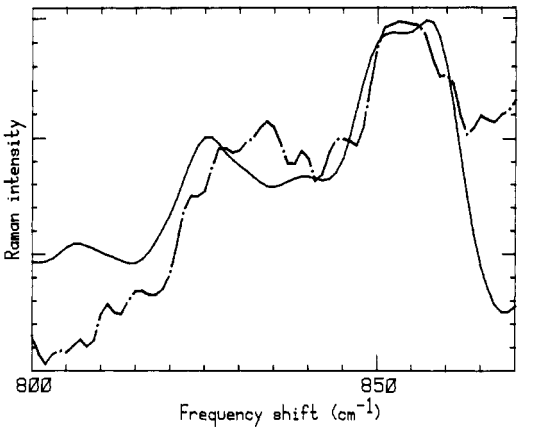

FIGURE 5: Tyrosine Raman spectrum of crambin crystals (solid line) and α_1-purothionin (dash with dot).

to change in integrated intensity relative to other bands during the crambin crystal to solution phase transition. The change in the amide III spectrum appears to be in the same amount and direction as the amide I change. An analysis of sequence secondary structure preference shows some ambiguity in the N-terminal end of the first helical segment of the homologous proteins, which is also consistent with the hypotheized difference in structures. Nevertheless, we cannot rule out the alternative explanations that intermolecular transition dipole coupling or removal of bound water at the solution to crystal transition may cause the observed differences. These results strengthen the motives for obtaining X-ray and Raman data from crystals of the purothionins.

Acknowledgments

We are greatly indebted to Dr. Richard Priest and Dr. Joel Schnur for their help with instrumentation at NRL, to Dr. Wayne Hendrickson for the results shown in Table IV, and to Dr. Janet Smith for helpful discussions.

Registry No. Tyrosine, 60-18-4.

References

Andersson, K., & Johannsson, M. (1973) *Eur. J. Biochem. 32*, 223–231.

Bandekar, J., & Krimm, S. (1980) *Biopolymers 19*, 31–36.

Bentley, G., Dodson, G., & Lewitova, A. (1978) *J. Mol. Biol. 126*, 871–875.

Carrasco, L., Vazquez, D., Hernandez-Lucus, C., Carbonero, P., & Garcia-Olmedo, F. (1971) *Eur. J. Biochem. 116*, 185–189.

Chang, C. T., Wu, C. S. C., & Yang, J. T. (1978) *Anal. Biochem. 91* 13–31.

Chou, P. Y., & Fasman, G. D. (1974a) *Biochemistry 13*, 211–222.

Chou, P. Y., & Fasman, G. D. (1974b) *Biochemistry 13*, 222–245.

Chou, P. Y. & Fasman, G. D. (1977) *J. Mol. Biol. 115*, 135–175.

Dodson, E. J., Dodson, G. G., Hubbard, R. E., & Reynolds, C. D. (1983) *Biopolymers 22*, 281–291.

Garnier, J., Osguthorpe, D. J., & Robson, B. (1978) *J. Mol. Biol. 120*, 97–120.

Hendrickson, W. A., & Teeter, M. M. (1981) *Nature (London) 290*, 107–113.

Honzatko, R. B., & Williams, R. W. (1982) *Biochemistry 21*, 6201–6205.

Jones, B. L., & Mak, A. S. (1977) *Cereal Chem. 54*, 511–523.

Krimm, S., & Bandekar, J. (1980) *Biopolymers 19*, 1–29.

Lawson, C. L., & Hanson, F. J. (1974) in *Solving Least Squares Problems*, Prentice-Hall, Englewood Cliffs, NJ.
Lesk, A. M., & Chothia, C. (1980) *J. Mol. Biol. 136*, 225–270.
Levitt, M. (1978) *Biochemistry 17*, 4277–4285.
Levitt, M., & Greer, J. (1977) *J. Mol. Biol. 114*, 181–293.
Mak, A. S., & Jones, B. L. (1976a) *Can. J. Biochem. 54*, 835–842.
Mak, A. S., & Jones, B. L. (1976b) *J. Sci. Food Agric. 27*, 205–213.
Matthews, B. W. (1976) *Annu. Rev. Phys. Chem. 27*, 493–523.
Moore, W. H., & Krimm, S. (1976) *Biopolymers 15*, 2439–2464.
Nemethy, G., Phillips, D. C., Leach, S. J., & Scheraga, H. A. (1967) *Nature (London) 214*, 363–365.
Okada, T., & Yoshizumi, H. (1973) *Agric. Biol. Chem. 37*, 2289–2294.
Okada, T., Yoshizumi, H., & Terashima, Y. (1970) *Agric. Biol. Chem. 34*, 1084–1094.
Richardson, J. S. (1981) *Adv. Protein Chem. 34*, 167–339.
Robson, B., & Suzuki, E. (1976) *J. Mol. Biol. 107*, 327–356.
Samuelsson, G., Seger, L., & Olson, T. (1968) *Acta Chem. Scand. 22*, 2624–2642.
Savitsky, A., & Golay, M. (1967) *Anal. Chem. 36*, 1627–1639.
Siamwiza, M. N, Lord, R. C., Chen, M. C., Takamatsu, T., Harada, I., Matsuura, H., & Shimanouchi, T. (1975) *Biochemistry 14*, 4870–4876.
Teeter, M. M., & Hendrickson, W. A. (1979) *J. Mol. Biol. 127*, 219–223.
Teeter, M. M., & Kossiakoff, A. A. (1982) in *Neutrons in Biology* (Schoenborn, V., Ed.) pp 335–348, Plenum Press, New York.
Teeter, M. M., Mazer, J. A., & L'Italien, J. J. (1981) *Biochemistry 20*, 5437–5443.
Van Etten, C. H., Nielsen, H. C., & Peters, J. E. (1965) *Phytochemistry 4*, 219–223.
Van Wart, H. E., & Scheraga, H. A. (1976a) *J. Phys. Chem. 80*, 1812–1823.
Van Wart, H. E., & Scheraga, H. A. (1976b) *J. Phys. Chem. 80*, 1823–1832.
Wallace, B. A., Kohl, N., & Teeter, M. M. (1984) *Proc. Natl. Acad. Sci. U.S.A. 81*, 1406–1410.
Williams, R. W. (1983) *J. Mol. Biol. 166*, 581–603.
Williams, R. W. (1985) *Methods Enzymol.* (in press).
Williams, R. W., & Dunker, A. K. (1981) *J. Mol. Biol. 152*, 738–813.
Williams, R. W., & Hendrickson, W. A. (1984) *FEBS Lett. 165*, 223–226.
Williams, R. W., Dunker, A. K., & Peticolas, W. L. (1980) *Biophys. J. 32*, 232–234.
Williams, R. W., Gaber, B. P., & Gunning, J. (1982) *J. Biol. Chem. 257*, 13321–13323.
Wooley, D. W., & Krampitz, L. O. (1942) *J. Biol. Chem. 146*, 273–274.

Time-Resolved Resonance Raman Study of Alkaline Isomerization of Ferricytochrome *c*†

Tadayuki Uno, Yoshifumi Nishimura, and Masamichi Tsuboi*

ABSTRACT: A transient intermediate in the course of alkaline isomerization reaction of ferricytochrome *c* has been detected by the use of a stopped-flow resonance Raman spectroscopy, when the pH of the reactant solution was jumped from 6.9 to 12.0. Resonance Raman lines at 1610 and 1640 cm^{-1} have been observed in the transient species. Resonance Raman spectra of totally guanidinated ferricytochrome *c* were also obtained at pH 7.2 and at pH 11.5. At the alkaline pH, the guanidinated derivative has resonance Raman lines at 1478, 1505, 1552, 1588, 1608, and 1637 cm^{-1}. From these frequencies it was suggested that its alkaline form has a structural similarity (around the heme environment) to the alkaline intermediate form of the native cytochrome *c*. This suggestion was supported by the absorption spectrum of the alkaline form of the guanidinated derivative, which has an intense 600-nm band and a blue-shifted Soret band. These Raman frequencies as well as those of the transient species of the native protein are interpreted to consist of high- and low-spin components. They indicate that the distance between the center of the porphyrin core and the pyrrole nitrogen is 2.07 Å for the high-spin component and 2.00 Å for the low-spin component (both of the alkaline form of the guanidinated ferricytochrome *c* and of the alkaline intermediate form of the native cytochrome *c*). Thus, the heme iron is considered to reside in the heme plane regardless of the spin state of the heme iron in these proteins.

Ferricytochrome *c* is known to take several different conformations depending on pH (Theorell & Åkesson, 1941). It undergoes a subtle conformational isomerization near pH 9. At neutral pH, it is in a low-spin state and has Met-80 as the sixth ligand. It has a weak absorption band at 695 nm, which is characteristic of sulfur ligation to the heme iron (Smith & Williams, 1970). As the pH is raised, the alkaline isomerization takes place, and the methionine ligand is replaced by a strong field ligand, which keeps the heme iron in a low-spin state. This new ligand is supposed to be Lys-79 or Lys-72 (Hettinger & Harbury, 1964; Gupta & Koenig, 1971; Davis et al., 1974; Wilgus & Stellwagen, 1974; Kitagawa et al., 1977a,b; Smith & Millett, 1980). By this transition, ferricytochrome *c* loses the reducibility (Greenwood & Palmer, 1965), its 695-nm band disappears, and the methyl signal of

† From the Faculty of Pharmaceutical Sciences, University of Tokyo, Hongo, Bunkyo-ku, Tokyo 113, Japan. *Received April 3, 1984.* This work was supported by Grant-in-Aid 57101003 from the Ministry of Education, Science, and Culture of Japan.

0006-2960/84/0423-6802$01.50/0